Theoretical deposition of nanotubes in the respiratory tract of children and adults

Robert Sturm

Brunnleitenweg 41, 5061 Elsbethen, Salzburg, Austria
Corresponding to: Dr. Robert Sturm. Brunnleitenweg 41, 5061 Elsbethen, Salzburg, Austria. Email: Robert.Sturm@stud.sbg.ac.at.

Introduction: Nanotubes are assumed to contribute to a significant exacerbation of asthma and to enhance the risk of profibrotic effects in lungs being affected by this injury. Therefore, deposition of nanotubes in the lungs of subjects with different ages was subject to a detailed theoretical investigation.

Methods: Nanoparticle deposition was computed by application of well validated stochastic deposition model, including four main deposition forces (Brownian diffusion, inertial impaction, interception, gravitational settling). Nonspherical particle geometry was considered with the help of the aerodynamic diameter concept. Deposition was calculated for particles with diameters adopting values of 1, 10, and 100 nm as well as aspect ratios of 10, 50, and 100. Lungs of subjects with different ages were generated with the help of scaling factors and allometric functions. Inhalation was uniformly supposed to take place under non-strain conditions (sitting breathing conditions).

Results: Total deposition of nanotubes is significantly increased with proceeding age, with deposition probability being negatively correlated with particle size (diameter and aspect ratio). Whilst extrathoracic deposition is subject to a slight decrease from infants to adults, bronchial/bronchiolar and alveolar depositions are exponentially increased.

Discussion and conclusions: Due to an increase of nanotube deposition with proceeding age infants and children enjoy a certain protection from excessive particle exposure. This circumstance mostly reprieves their lungs from injuries induced by this sort of particles.

Keywords: Nanoparticles; deposition; lung; Monte-Carlo model; stochastic model; lung deposition; Brownian diffusion; asthma

Introduction

During the last decades nanotubes made of carbon have become manufacturing materials of immense importance due to their high electric conductivity, their mechanical strength, and their ability to undergo a derivatization for custom applications. These unique characteristics make nanotubes highly desirable in electronics, structural engineering, and medicine (1,2). Concerning their size carbon nanotubes range from one to several nanometers in width and measure up to several micrometers in length. Therefore, the length to width (aspect) ratio of these highly specific particles may reach values up to 1,000 which results in a similarity of their behaviour in the air to that of asbestos fibers. Once inhaled into the human respiratory tract, carbon nanotubes may cause asbestos-like insufficiencies of the lungs such as pulmonary inflammation, pulmonary fibrosis and lung cancer (2,3).

Recent studies (4-6) have yielded evidence that nanoparticles (including nanotubes) with a mass median aerodynamic diameter less than 0.1 μm may significantly affect the cardiopulmonary system. Basically, they are marked by a larger surface area with respect to particles of μm-size and the ability to penetrate into deeper parts of the respiratory system, where they may cause an

enhanced inflammatory response (7,8). In the case of carbon nanotubes consisting of multiple walls it has been additionally postulated that adverse effects of these particles may be manifested under the conditions of pre-existing inflammation such as allergic asthma (1,9). Regarding its pathogenesis asthma involves a chronic re-modeling of the lung airways which is commonly accompanied by eosinophilic inflammation, mucus hypersecretion from glands of the bronchial epithelium, thickening of the airway smooth muscle cells, and airway fibrosis (10). From recent epidemiologic studies (11,12) we have obtained knowledge that the nanoscale fraction of airborne particulate matter is most significant to the exacerbation of asthma and that patients suffering from this injury are at greater risk for profibrotic effects of such nanomaterials.

Since inhalation experiments using nanomaterials are restricted to labour animals for many ethical reasons, there is only limited information with regard to the transport, deposition, and clearance of such particulate matter in the human respiratory system. During the last 20 years theoretical models, being subjected to multiple processes of validation, have helped to overcome this deficit of knowledge (13-18). Current mathematical approaches to the depositon of spherical or nonspherical nanoparticles in the respiratory tract postulate a dependence of the main deposition sites upon a rather wide spectrum of physical and physiological parameters. These among other include numerous properties of the particles themselves (geometry, density, *etc*.) as well as the breathing conditions (inhalation time, tidal volume, *etc*.) during inhalative particle uptake (13-15). Generally, nanoparticles with a mass median aerodynamic diameter less than 10 nm are most effectively filtered in the uppermost regions of the respiratory system, whilst particles ranging in mass median aerodynamic diameter from 10 to 100 nm are preferably deposited in intermediate to distal lung regions (13). The ability of ultrafine particles to penetrate to deeper lung compartments positively correlates with the inspired air volume V_t and the inhalative flow rate Q (14,15). Concerning the clearance of nanoparticles and especially those with nonspherical geometry from the respiratory tract theoretical approaches still run through a process of further experimental validation and refinement. However, it is postulated that in principle nanoparticles are affected by the same clearance mechanisms as larger particles, whereby some of these mechanisms such as particle uptake by macrophages are reduced, whilst others such as transepithelial transport are enhanced (16-18).

The present study aims to increase the current theoretical knowledge of nanoparticle deposition in the human respiratory tract by investigating respective deposition scenarios of variably sized particles in the lungs of infants (1 year), children (5 years), adolescents (15 years), and adults (>20 years).

Material and methods

Theoretical model of lung morphometry

Lung morphometry was approximated by application of the stochastic geometric model formerly introduced by Koblinger and Hofmann (19,20). This approach consists of an extensive statistical treatment of lung morphometric data obtained from interferometric measurements of the tracheobronchial tree (21) and the acinar lung compartment (22). Construction of tracheobronchial architecture is conducted by the selection of essential geometric parameters such as airway diameters, airway lengths, branching angles, and gravity angles from lung generation-specific probability density functions. This selection is realized with the help of a pseudo-random generator. During this mathematical process also essential correlations between the morphometric parameters themselves are considered. The procedure ends in the construction of random airway paths as well as the arrangement of a pre-selected number of these paths (e.g., 10,000) to a stochastic lung.

In the original stochastic lung model proposed by Koblinger and Hofmann (20) size of the tracheobronchial tree was calibrated to a functional residual capacity (FRC) of 3,300 mL, representing the mean value of this volume parameter for a male Caucasian adult (23). Children's and adolescents' lung morphometries were approximated by an appropriate re-calibration of the tracheobronchial tree using respective scaling factors. According to Phalen *et al.* (24) dimensions of the trachea and bronchi correspond to body height in the following way:

$$SF = a \cdot (Hs - 1.76) + 1 \qquad [1]$$

Within Eq. [1] *SF* denotes the scaling factor, i.e., the ratio of airway diameter or length in the subject of interest compared to that in reference man. H_S represents the height of the subject of interest in meters, whereas *a* yields an airway generation-specific constant (23). As a useful alternative to Eq. [1] scaling factors for airway diameters

Table 1 Scaling and breathing parameters of the age groups investigated in the present paper

	1y	5ys	15ys	adult
SF	0.353	0.517	0.780	0.840
FRC (mL)	244	767	2,650	3,300
TV (mL)	102	213	625	750
BF (min⁻¹)	43.2	30.0	18.5	14.4
T (s)	1.39	2.00	3.24	4.17
BH (s)	0.00	0.00	0.50	1.00

SF, scaling factor; FRC, functional residual capacity; TV, tidal volume; BF, breathing frequency; T, length of breath cycle; BH, breath-hold time.

and lengths of the tracheobronchial tree may be computed according to the mathematical formula:

$$SF = \sqrt[3]{\frac{FRC_S}{FRC_R}} \qquad [2]$$

with FRC_S denoting the functional residual capacity of the subject of interest and FRC_R representing the functional residual capacity of a reference subject (23). Values of airway re-calibration computed with Eq. [2] are summarized together with age-specific physiological parameters necessary for modelling computations in *Table 1*.

Modelling particle deposition in lungs of different age

Deposition of particles in the respiratory tract of humans with different age was computed by the application of analytical deposition equations that (I) commonly describe the effect of four main deposition forces (Brownian diffusion, inertial impaction, interception, and gravitational settling) and (II) are only valid for straight cylindrical tubes and spheres. Regarding particle deposition by Brownian diffusion the respective empirical equation proposed by Cohen and Asgharian (23) was used. This theoretical approach assumes an increase in deposition in the upper bronchial airways due to developing flow. For diffusion-induced particle deposition in more peripheral airway tubes the empirical equation outlined by Ingham (25) was applied. Proximal particle deposition due to inertial impaction and interception was mainly approximated by the use of correction factors which were added to the standard

equations (26). Deposition in the extrathoracic region, expressing the ability of oral and nasal airways to filter out the inhaled material, was also calculated with the help of empirical equations that either had been derived from *in vivo* measurements or had been collected from experimental data.

Analytical and empirical deposition formulae noted above are commonly founded on the hypothesis of ideally spherical particles being inhaled from the ambient atmosphere. However, most aerosol particles emanating from natural or anthropogenic sources significantly deviate from this spherical geometry and occur with fibrous or disk-like shapes. Such nonspherical particles often represent serious health hazards, especially when they are inspired by children (27). In some cases aerosols are not composed of single particles but consist of irregularly shaped aggregates which themselves are composed of high numbers of randomly arranged spherical or nonspherical components (28).

In general, nonspherical particle geometries are most reliably approximated with the help of the aerodynamic diameter concept (mobility diameter for ultrafine particles). The aerodynamic diameter, d_{ae}, corresponds to the diameter of a unit-density sphere with exactly the same aerodynamic characteristics as the nonspherical particle of interest. From a mathematical point of view, d_{ae} is defined by the formula (28-30):

$$d_{ae} = \sqrt{\frac{1}{\chi} \cdot \frac{\rho_P}{\rho_0} \cdot \frac{C_{d_{ve}}}{C_{d_{ae}}}} \qquad [3]$$

with χ yielding the dynamic shape factor, ρ_P the density of the particle, ρ_0 unit density (1 g·cm⁻³), $C_{d(ve)}$ the Cunningham correction factor for a spherical particle with volume equivalent diameter, and $C_{d(ae)}$ the Cunningham correction factor for a particle with respective aerodynamic diameter. Estimation of χ, $C_{d(ve)}$, and $C_{d(ae)}$ is conducted according to mathematical standard procedures introduced in numerous previous publications (28-30).

Results

Computation of age-dependent lung morphometry and breathing behaviour

Main characteristics of lung morphometry among the different age groups are presented by plotting lung generation-specific airway diameters against respective lung
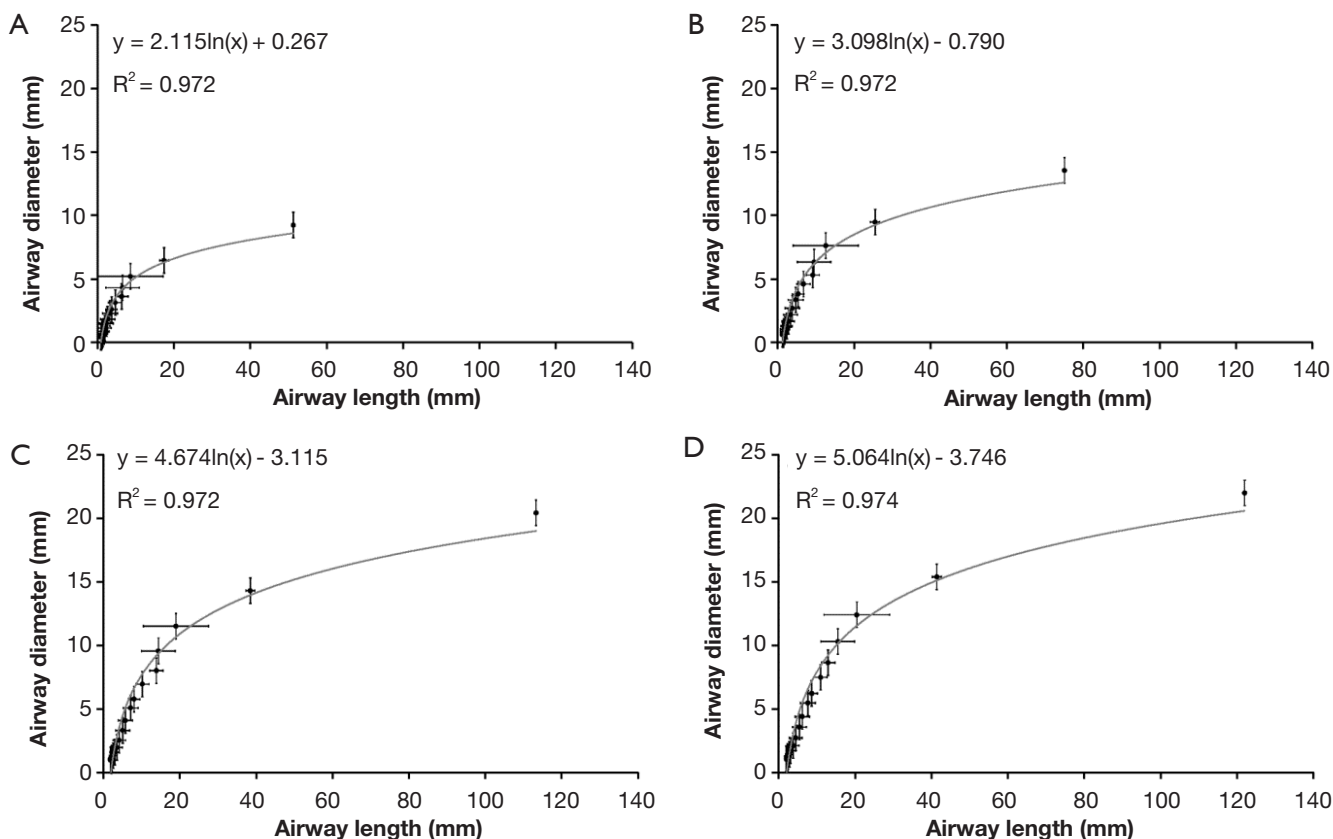
Figure 1 Logarithmic relation between airway diameter (mm) and airway length (mm) for lung generations 1 (trachea) to 12: (A) 1-year old infant; (B) 5-year old child; (C) 15-year old adolescent; (D) adult. Logarithmic regression functions and goodnesses of fit (R²) are additionally provided.

generation-specific airway lengths (*Figure 1*). Independent of the age group considered in this context, airway diameter and airway length correlate according to a logarithmic function of the form $y = a \cdot ln(x) + b$. In all investigated cases goodness-of-fit, R^2, ranges from 0.972 to 0.974. Shapes of the generated functions are identical due to the application of scaling factors. As provided by the respective graphs, airway diameters of infants range from 7.8±0.6 mm (trachea) to 0.83±0.07 mm (lung generation 12). Airway lengths, on the other hand, vary between 39.7±1.3 mm (trachea) and 4.2±0.14 mm (lung generation 12). In 5-year old children airway diameters and lengths increase in size by a factor of 1.46, which corresponds to an enlargement of the lung of nearly 50%. Comparison of lungs of 15-year old adolescents with those of 5-year old children reveals a further increase of airway diameters and lengths by a factor of 1.37. Between infants and adolescents the lungs are subject to a 221% enlargement. Within the last growth stage taking place between adolescent and adult age the lung airways are further enlarged in diameter and length by a factor of 1.08.

With respect to infant lungs these fully developed lungs are enlarged by 238%.

Regarding the development of the scaling factor, diverse lung volumes, and breathing behaviour respective computational results are summarized in *Figure 2*. The dependences of these parameters upon subject's age are best presented by a polynomial of degree 2, with goodness-of-fit, R^2, ranging from 0.984 to 1.000. Increase of scaling factor and tidal volume with subject age commonly takes place according to a convexly shaped function, whilst increase of breath-cycle time with subject age commonly follows a concave function curve and functional residual capacity is almost linearly enhanced with subject age.

Deposition of nanotubes with variable size and its dependence on subject's age

Concerning the deposition of variably sized nanotubes in the human respiratory tract of subjects with different age the following distinctions have been carried out: (I) subject's
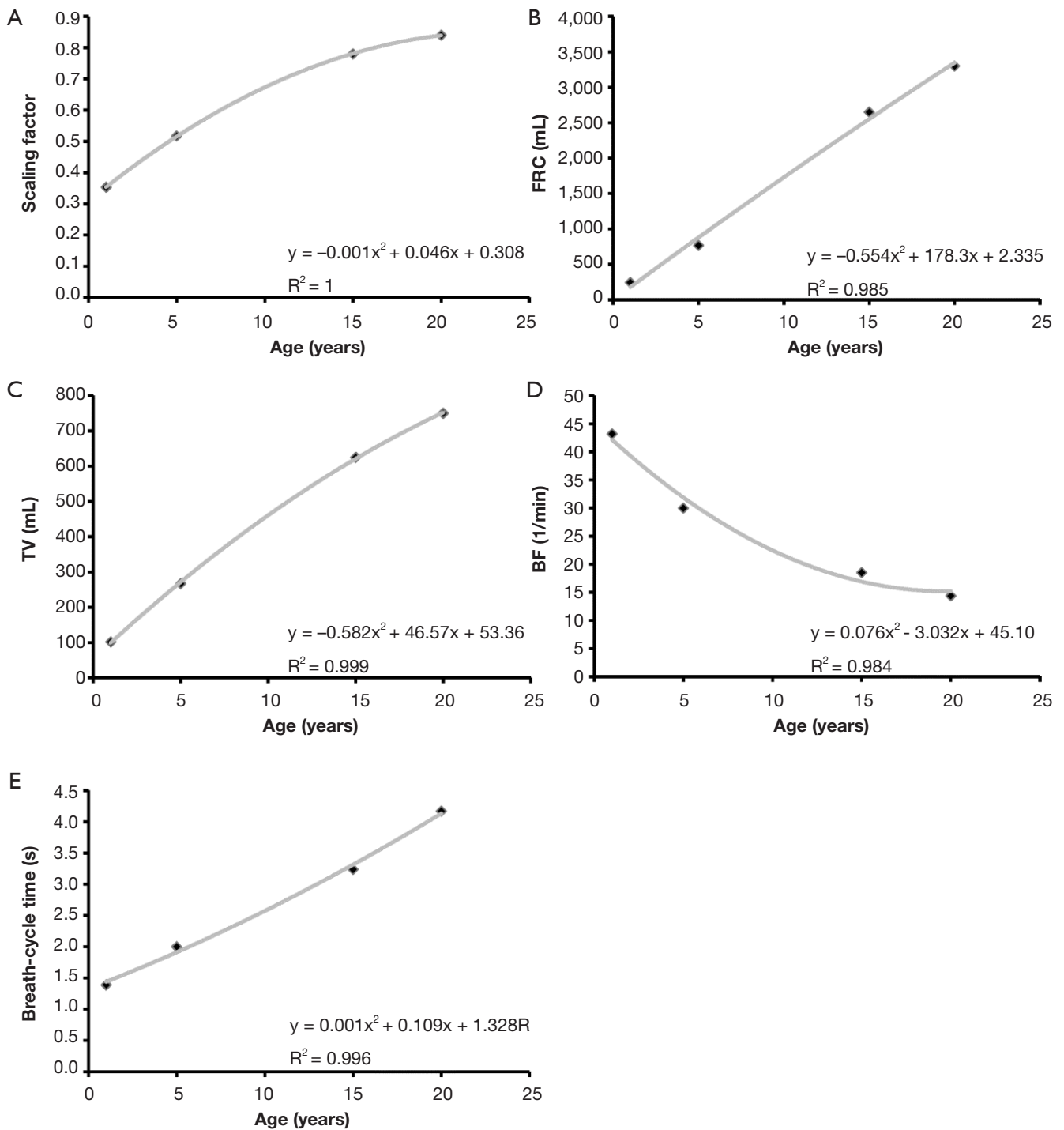
Figure 2 Age dependence of the lung scaling factor as well as diverse breathing parameters: (A) scaling factor; (B) functional residual capacity (FRC); (C) tidal volume (TV); (D) breathing frequency (BF); (E) breath-cycle time. Second-grade polynomial regression functions and goodnesses of fit (R^2) are additionally provided.

age was continuously observed, starting with 1-year old infants and ending with 20-year old adults; (II) besides total particle deposition including the deposition of nanotubes in all compartments of the respiratory tract, also extrathoracic, bronchial/bronchiolar, and alveolar deposition of nanotubes was computed; (III) nanotubes were assumed to have perfect cylindrical shape with respective cylindrical diameters adopting values of 1, 10, and 100 nm. Related aspect ratios of the tubes were set to 10, 50, and 100; (IV) breathing of the subjects was supposed to take place without any physical strain (23). Results of the simulations are illustrated in the graphs of *Figures 3-6*.

Total deposition of nanotubes is commonly characterized by a logarithmic increase with proceeding subject age (*Figure 3*). Highest deposition probabilities are computed for nanotubes with 1 nm diameter, followed by those with 10 nm diameter and those with 100 nm diameter. Any increase of the aspect ratio leads to a decline of total deposition, so that very long tubes (β=100) produce total deposition probabilities less than 15%. Highest values for total deposition may be attested for nanotubes with a diameter of 1 nm and a length of 10 nm that have been inhaled by adult subjects (>80%).

Extrathoracic deposition of nanotubes is generally subject to a decrease with proceeding subject age, whereby deposition behaviour of the inhaled particles is very similar to that outlined for total deposition. This means that smaller particles with minimal diameters and aspect ratios exhibit higher deposition probabilities than larger particles with maximal diameters and aspect ratios (*Figure 4*). For smallest nanotubes deposition probability usually ranges from 15% to 40%, whilst for largest particles deposition probability varies between 1.0% and 1.8%.

With regards to bronchial and bronchiolar deposition some interesting observations can be made (*Figure 5*): first, deposition probability is subject to an exponential, partly steep increase with proceeding subject age; second, smallest particles are deposited with few percent in infants' bronchi and bronchioli, but with up to 63% in the airway tubes of adults. The lengths of the nanotubes do not show any significant effects on deposition behaviour; third, deposition probability of intermediately sized and large nanotubes is continuously reduced and is limited to few percent in infants and children; fourth, nanotubes with a diameter of 100 nm and an aspect ratio of 10 behave very similar to nanotubes with a diameter of 100 nm and an aspect ratio of 100.

Alveolar deposition of nanotubes is characterized by

the circumstance that numbers of deposited particles are subject to a steep increase from 1- to 5-year old subjects and an intermediate increase from 6- to 20-year old subjects. Nanotubes with a diameter of 1 nm exhibit a maximal deposition probability of 5%, whereby number of deposited particles is continuously declined with increasing aspect ratio (*Figure 6*). For nanotubes with a diameter of 10 nm, deposition probability and aspect ratio are positively correlated, whereas for nanotubes with a diameter of 100 nm highest aspect ratios generate highest deposition probabilities.

Discussion and conclusions

In the past decades nanoparticles have excited enhanced scientific interest for several kinds of reasons: first, not much information on the behaviour of such particles within the inhaled air stream was available hitherto; second, the effects of these ultrafines on the lung epithelium, lung parenchyma and lung-associated tissues was largely unknown. Experimental studies carried out on laboratory animals (31,32) as well as theoretical investigations (33,34) have successively helped to overcome this deficit of knowledge. Today it is a widely accepted paradigm that nanoparticles may be responsible in part for the exacerbation of diverse lung injuries, but may also induce cardiovascular insufficiencies due to their ability of being transported and accumulated in the blood capillaries within rather short periods of time (35,36).

Whilst nanoparticles of natural origin are rarely found in the ambient atmospheric concentrations of artificial nanoparticles have been continuously increased in the last years. This is mainly due to an exponential growth of traffic producing ultrafine soot from combustion processes and the introduction of innovative nanomaterials which besides their industrial use may act as potential health hazards (35). The main problem with regards to nanoparticles is their significant deviation from ideal, spherical geometries, complicating any predictions of their deposition in the human respiratory system immensely. As found by microscopic studies soot particles form aggregates of highly irregular shape (15,30), affecting their aerodynamic behaviour significantly. Nanomaterials, on the other hand, consist of single- or multi-walled carbon tubes, whose aerodynamic characteristics are largely comparable with those of asbestos fibers (1-3).

Theoretical concepts for a reliable modeling of irregular particle shapes have been a point of extensive scientific
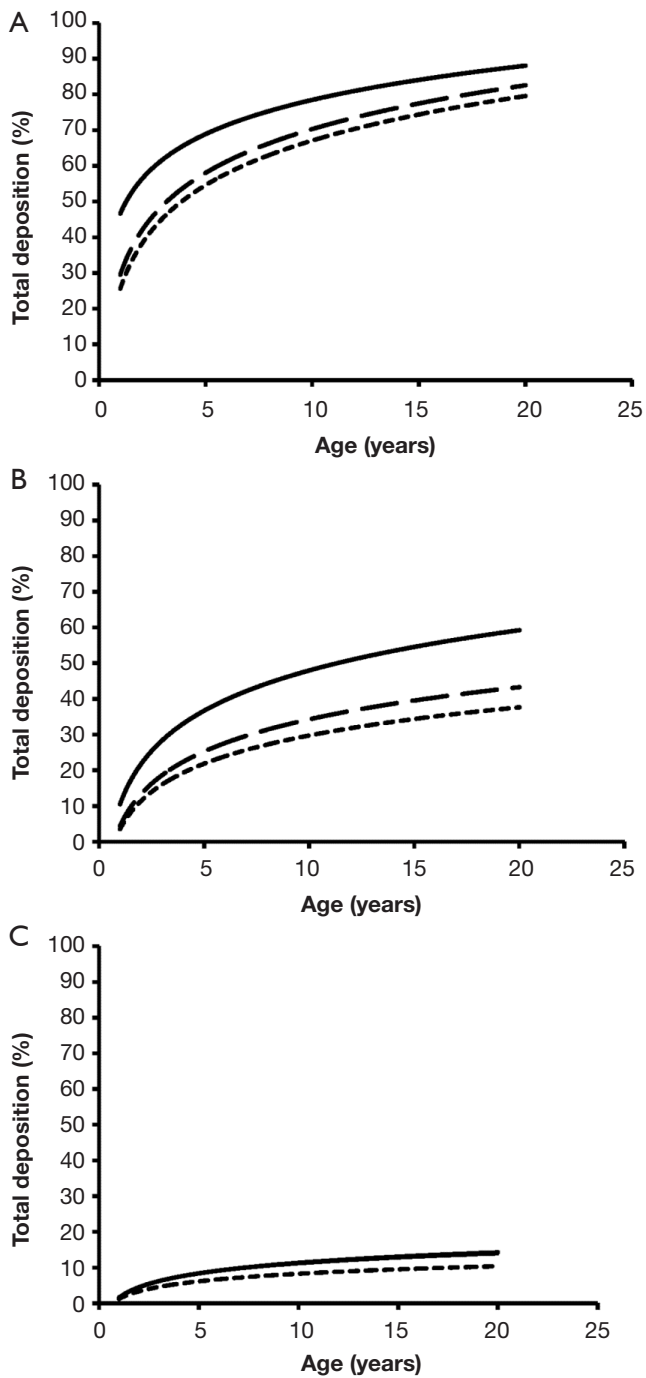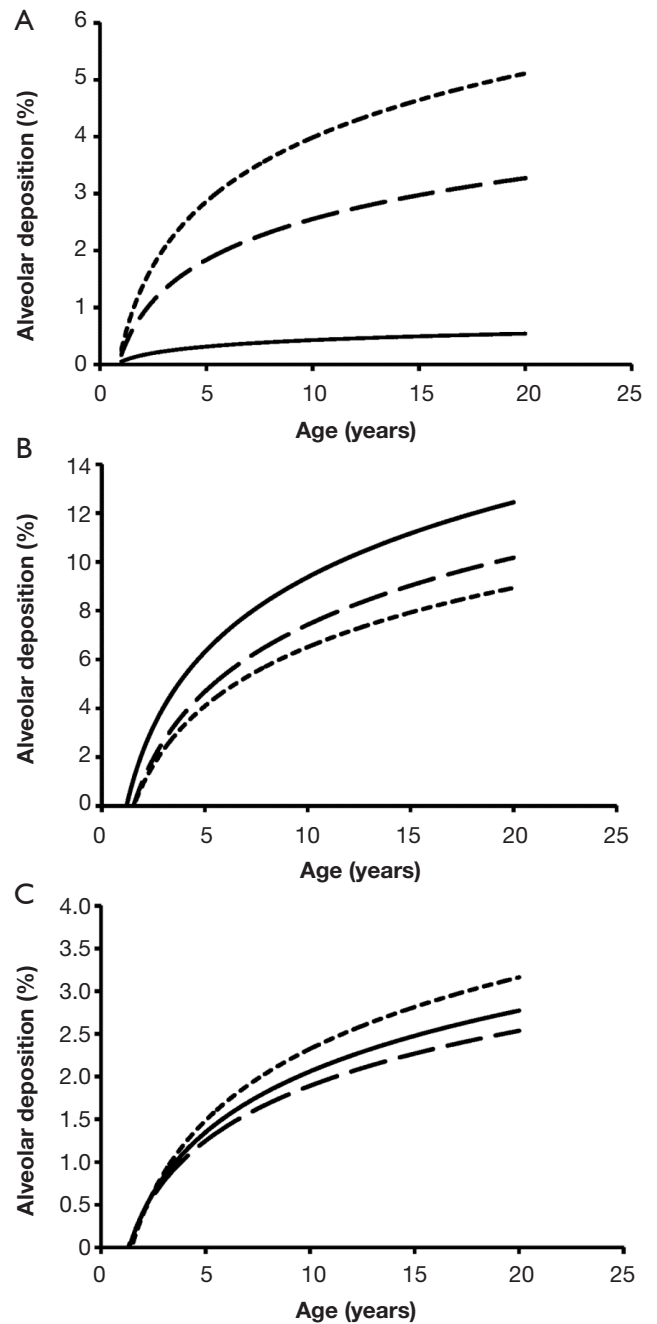
Figure 3 Age dependence of total nanotube deposition in the respiratory tract: (A) tubes with 1 nm diameter; (B) tubes with 10 nm diameter; (C) tubes with 100 nm diameter. Solid lines yield an aspect ratio β of the tubes of 10, dashed lines an aspect ratio of 50, and dotted lines an aspect ratio of 100.
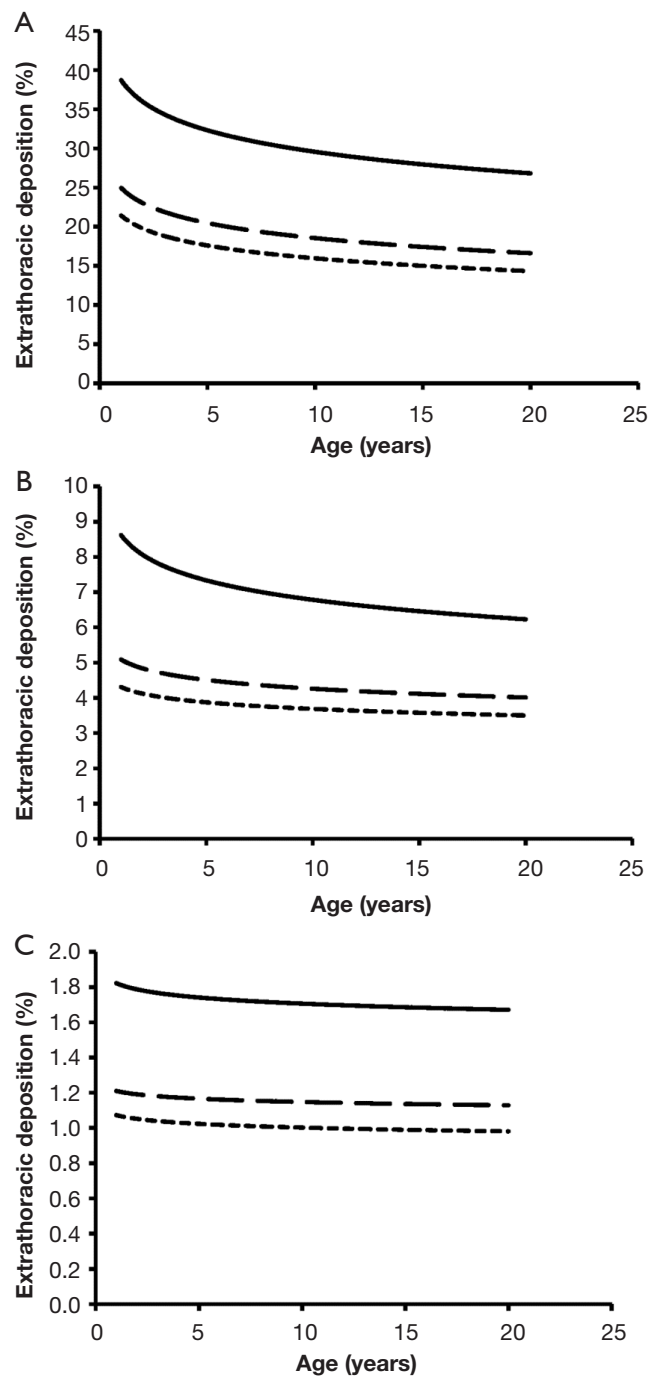
Figure 4 Age dependence of extrathoracic nanotube deposition in the respiratory tract: (A) tubes with 1 nm diameter; (B) tubes with 10 nm diameter; (C) tubes with 100 nm diameter. Solid lines yield an aspect ratio β of the tubes of 10, dashed lines an aspect ratio of 50, and dotted lines an aspect ratio of 100.
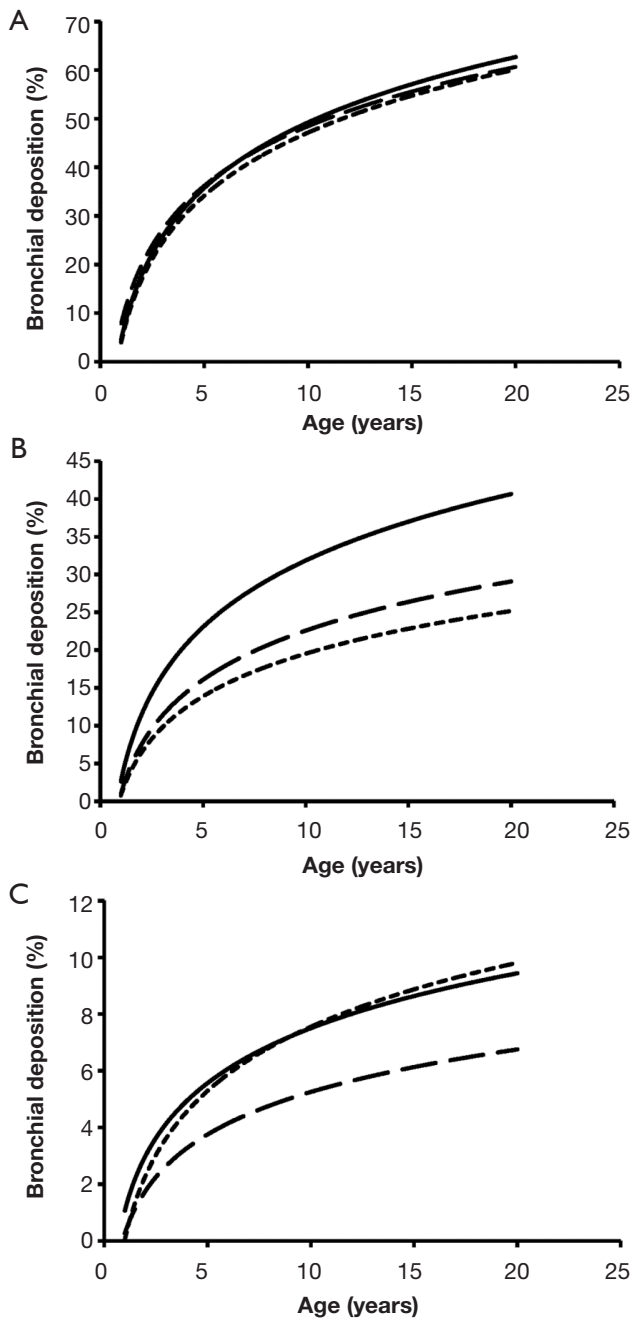
Figure 5 Age dependence of bronchial nanotube deposition in the respiratory tract: (A) tubes with 1 nm diameter; (B) tubes with 10 nm diameter; (C) tubes with 100 nm diameter. Solid lines yield an aspect ratio β of the tubes of 10, dashed lines an aspect ratio of 50, and dotted lines an aspect ratio of 100.

Figure 6 Age dependence of alveolar nanotube deposition in the respiratory tract: (A) tubes with 1 nm diameter; (B) tubes with 10 nm diameter; (C) tubes with 100 nm diameter. Solid lines yield an aspect ratio β of the tubes of 10, dashed lines an aspect ratio of 50, and dotted lines an aspect ratio of 100.

debate during the past forty years; meanwhile highest acceptance is given to the approach initially introduced by Stöber in the 1970s, using the dynamic shape factor and aerodynamic diameter of a nonspherical particle (28). Most current mathematical models attempt the construction of realistic nanoparticles with the help of fractal geometry (34), but are still unsuited for any establishment in widely used particle deposition codes.

Early models of the lungs such as that introduced by Weibel in the 1960s (37) were restricted to the description of tracheobronchial airway architecture and morphometry of adults. Since the fundamental contribution of Menache *et al.* (38) we possess increased knowledge of the child's respiratory system and its main discrepancies from the adult lungs. For microdosimetric examinations lungs of humans from 1 year (infants) to 15 years (adolescents) in age were modelled by application of allometric equations and scaling factors resulting from partly extensive morphometric studies (23). Based on these fundamentals on the one hand and numerous theoretical computations conducted in the past decade (23,27,39) on the other hand, it has been found that particle deposition in children's lungs may differ significantly from that in adults' lungs.

As presented in the graphs of *Figures 3-6*, deposition of nanotubes in the human respiratory tract may indeed be regarded as a function depending on subject's age. Whilst extrathoracic deposition exhibits a negative correlation with subject's age, total, bronchial, and alveolar deposition show a theoretical increase with proceeding subject's age. However, it has to be noted that this deposition behaviour of nanotubes has been investigated for subjects ranging from 1 year to 20 years in age and thus can only give coarse predictions for older subjects (>50 years in age). This is mainly due to the fact that breathing behaviour of older subjects may differ significantly from that of younger ones (23). Differences of nanotube deposition among the age groups investigated for this study are based upon three main reasons: first, nanotubes, especially those with low aspect ratios, are deposited on the walls of the respiratory system due to their continuous collisions with air molecules (Brownian motion); second, this deposition by Brownian motion describing the radial displacement of particles in the air stream is enhanced in subjects with smaller lung morphometry; third, deposition by Brownian motion becomes more effective, if nanoparticles transported in the inhaled air stream are characterized by longer residence times within the respiratory system (e.g., by enhanced duration of the breathing cycle or intercalation of pauses

between inhalation and exhalation) or penetration of such particles into deeper lung regions is enabled (e.g., by an increase of the tidal volume) (23,27). In the respiratory system of infants and children significantly reduced airway calibers and lengths may favour nanotube deposition on the one hand, but, on the other hand, shallow breathing, being typical for these age groups, minimizes particle residence times in the airway system. High extrathoracic deposition fractions may be explained by the circumstance that oral and nasal air passages of children are reduced in size compared to the respective passages in adolescents and adults and thus nanoparticles, being radially dispersed during their two-way transport through the thoracic airways, finally collide with the extrathoracic airway walls.

With increasing diameter of the nanotubes deposition observed for the single age groups is commonly subject to a remarkable decrease. This phenomenon is caused by the fact that Brownian motion continuously loses its significance with increasing particle size, but, on the other side, deposition forces such as inertial impaction, interception, and gravitational settling require even larger particles to unfold their optimal efficiencies (14-20). Hence, particles reach aerodynamic diameters being more and more characterized by minimal effects of deposition forces (23). A similar effect may be observed with increasing aspect ratio of the nanotubes, also reflecting an enhancement of the aerodynamic diameter. An exception to this rule is given for alveolar deposition exhibited in *Figure 6*, where nanotubes of intermediate size are marked by highest deposition values. Particles belonging to this size category have an increased ability to penetrate to the pulmonary compartment of the lungs, where they undergo alveolar mixing and, as a consequence of that, may collide with the alveolar walls. Larger particles are less forced to deposition by the alveolar mixing process.

From the results provided in this study it may be concluded that nanotubes may become serious health hazards and, in the worst case, also triggers of malignant transformation. This circumstance depends upon the (I) effective size of the nanotubes and (II) the intensity of particle inhalation. Although particle deposition scenarios are simulated with high accuracy meanwhile, further refinements of respective deposition models have to be done in near future.

Acknowledgements

References

1. Donaldson K, Aitken R, Tran L, et al. Carbon nanotubes: a review of their properties in relation to pulmonary toxicology and workplace safety. Toxicol Sci 2006;92:5-22.

2. Ryman-Rasmussen JP, Tewksbury EW, Moss OR, et al. Inhaled multiwalled carbon nanotubes potentiate airway fibrosis in murine allergic asthma. Am J Respir Cell Mol Biol 2009;40:349-58.

3. Poland CA, Duffin R, Kinloch I, et al. Carbon nanotubes introduced into the abdominal cavity of mice show asbestos-like pathogenicity in a pilot study. Nat Nanotechnol 2008;3:423-8.

4. Peters A, Wichmann HE, Tuch T, et al. Respiratory effects are associated with the number of ultrafine particles. Am J Respir Crit Care Med 1997;155:1376-83.

5. Utell MJ, Frampton MW. Acute health effects of ambient air pollution: the ultrafine particle hypothesis. J Aerosol Med 2000;13:355-9.

6. Inoue K, Takano H, Yanagisawa R, et al. Effects of nano particles on antigen-related airway inflammation in mice. Respir Res 2005;6:106.

7. Li XY, Brown D, Smith S, et al. Short-term inflammatory responses following intratracheal instillation of fine and ultrafine carbon black in rats. Inhal Toxicol 1999;11:709-31.

8. MacNee W, Donaldson K. How can ultrafine particles be responsible for increased mortality? Monaldi Arch Chest Dis 2000;55:135-9.

9. Mitchell LA, Gao J, Wal RV, et al. Pulmonary and systemic immune response to inhaled multiwalled carbon nanotubes. Toxicol Sci 2007;100:203-14.

10. Brewster CE, Howarth PH, Djukanovic R, et al. Myofibroblasts and subepithelial fibrosis in bronchial asthma. Am J Respir Cell Mol Biol 1990;3:507-11.

11. Gavett SH, Koren HS. The role of particulate matter in exacerbation of atopic asthma. Int Arch Allergy Immunol 2001;124:109-12.

12. Matsumoto A, Hiramatsu K, Li Y, et al. Repeated exposure to low-dose diesel exhaust after allergen challenge exaggerates asthmatic responses in mice. Clin Immunol 2006;121:227-35.

13. Sturm R, Hofmann W. A computer model for the simulation of fiber deposition in the human respiratory tract. Comput Biol Med 2006;36:1252-67.

14. Sturm R. Deposition and cellular interaction of cancer-inducing particles in the human respiratory tract: Theoretical approaches and experimental data. Thoracic

15. Cancer 2010;4:141-52.

15. Sturm R. Theoretical models for dynamic shape factors and lung deposition of small particle aggregates originating from combustion processes. Z Med Phys 2010;20:226-34.

16. Sturm R, Hofmann W. Mechanistic interpretation of the slow bronchial clearance phase. Radiat Prot Dosimetry 2003;105:101-4.

17. Hofmann W, Sturm R. Stochastic model of particle clearance in human bronchial airways. J Aerosol Med 2004;17:73-89.

18. Sturm R, Hofmann W. A theoretical approach to the deposition and clearance of fibers with variable size in the human respiratory tract. J Hazard Mater 2009;170:210-8.

19. Koblinger L, Hofmann W. Analysis of human lung morphometric data for stochastic aerosol deposition calculations. Phys Med Biol 1985;30:541-56.

20. Koblinger L, Hofmann W. Monte Carlo modeling of aerosol deposition in human lungs. Part I: Simulation of particle transport in a stochastic lung structure. J Aerosol Sci 1990;21:661-74.

21. Raabe OG, Yeh HC, Schum GM, et al. Tracheobronchial geometry: human, dog, rat, hamster. Lovelace Foundation Report LF-53. Albuquerque: Lovelace Foundation, NM, 1976.

22. Haefeli-Bleuer B, Weibel ER. Morphology of the human pulmonary acinus. Anat Rec 1988;220:401-14.

23. International Commission on Radiological Protection (ICRP). Human respiratory tract model for radiological protection, Publication 66. Oxford: Pergamon Press, 1994.

24. Phalen RF, Oldham MJ, Beaucage CB, et al. Postnatal enlargement of human tracheobronchial airways and implications for particle deposition. Anat Rec 1985;212:368-80.

25. Ingham DB. Diffusion of aerosol from a stream flowing through a cylindrical tube. J Aerosol Sci 1975;6:125-32.

26. Yeh HC, Schum GM. Models of the human lung airways and their application to inhaled particle deposition. Bull Math Biol 1980;42:461-80.

27. Sturm R. Theoretical models of carcinogenic particle deposition and clearance in childrens lungs. J Thorac Dis 2012;4:368-76.

28. Stöber W. Dynamic shape factors of nonspherical aerosol particles. In: Mercer TT, Morrow PE, Stober W. eds. Assessment of airborne particles. Springfield: Charles C Thomas Publisher, 1972:249-89.

29. Davies CN. Particle-Fluid Interaction. J Aerosol Sci 1979;10:477-513.

30. Kasper G. Dynamics and measurement of smokes. I Size

characterization of nonspherical particles. Aerosol Sci Technol 1982;1:187-99.

31. Brain JD. Animal studies with environmental aerosols. J Aerosol Med 1993;6:33-7.

32. Mauderly JL, Gillett NA, Henderson RF, et al. Relationships of lung structural and functional changes to accumulation of diesel exhaust particles. Ann Occup Hyg 1988;32:659-68.

33. DeCarlo PF, Slowik JG, Worsnop DR, et al. Particle Morphology and Density Characterization by Combined Mobility and Aerodynamic Diameter Measurements. Part 1: Theory. Aerosol Sci Technol 2004;38:1185-205.

34. Katrinak KA, Rez P, Perkes PR, et al. Fractal geometry of carbonaceous aggregates from an urban aerosol. Environ Sci Technol 1993;27:539-47.

35. Bayram H, Ito K, Issa R, et al. Regulation of human lung epithelial cell numbers by diesel exhaust particles. Eur Respir J 2006;27:705-13.

36. Bayram H, Devalia JL, Sapsford RJ, et al. The effect of diesel exhaust particles on cell function and release of inflammatory mediators from human bronchial epithelial cells in vitro. Am J Respir Cell Mol Biol 1998;18:441-8.

37. Weibel ER. eds. Morphometry of the Human Lung. Berlin: Springer, 1963.

38. Ménache MG, Hofmann W, Ashgarian B, et al. Airway geometry models of children's lungs for use in dosimetry modeling. Inhal Toxicol 2008;20:101-26.

39. Sturm R. Age-dependence and intersubject variability of tracheobronchial particle clearance. Pneumon 2011;24:77-85.